NARMAX Representation and Identification of Ankle Dynamics

Sunil L. Kukreja, Henrietta L. Galiana, *Fellow, IEEE*, and Robert E. Kearney*, *Fellow, IEEE*

***Abstract*—Representation and identification of a parallel pathway description of ankle dynamics as a model of the nonlinear autoregressive, moving average exogenous (NARMAX) class is considered. A nonlinear difference equation describing this ankle model is derived theoretically and shown to be of the NARMAX form. Identification methods for NARMAX models are applied to ankle dynamics and its properties investigated via continuous-time simulations of experimental conditions. Simulation results show that 1) the outputs of the NARMAX model match closely those generated using continuous-time methods and 2) NARMAX identification methods applied to ankle dynamics provide accurate discrete-time parameter estimates. Application of NARMAX identification to experimental human ankle data models with high cross-validation variance accounted for.**

***Index Terms*—Ankle dynamics, mathematical modeling, NARMAX, nonlinear systems, system identification.**

I. Introduction

TRADITIONAL approaches to nonlinear system identification of human ankle dynamics have relied on quasilinear methods, e.g., impulse response method [1]. These methods provide a convenient, robust means of characterizing the dynamics of nonlinear systems without requiring *a priori* assumptions regarding the system structure. However, so-called nonparametric techniques may require many parameters to describe even simple systems and can be difficult to relate to the structure and parameters of the underlying physiological system [2].

Leontaritis and Billings [3], [4] have proposed the nonlinear autoregressive, moving average exogenous (NARMAX) structure as a general parametric form for modeling nonlinear systems. NARMAX models describe nonlinear systems in terms of linear-in-the-parameters difference equations relating the current output to (possibly nonlinear) combinations of inputs and past outputs. It is suitable for modeling both the stochastic and deterministic components of a system and is capable of describing a wide variety of nonlinear systems [5], [6]. This formulation yields compact model descriptions that may be readily identified and may afford greater interpretability.

Although the NARMAX structure is well suited to modeling the input–output (I/O) behavior of a physiological system, to date it has been used mainly for control where the main objective is to achieve a parsimonious system description. In biological modeling the objective is more often to gain insight into the function of the underlying system. Therefore, in this paper, we 1) theoretically analyze a nonlinear parallel pathway model of ankle dynamics to derive its NARMAX representation, 2) assess the applicability of this nonlinear model for the identification of biological systems, and 3) investigate the suitability of NARMAX identification methods applied to ankle dynamics.

Our results show that the NARMAX model class is well suited to modeling the I/O behavior of a parallel pathway model describing ankle dynamics. Identification results illustrate that methods for identification of NARMAX models are well suited for identifying ankle dynamics. Analysis of experimental data using NARMAX identification techniques provides a parameter set that explains the I/O data well. Overall, this paper contributes to the understanding of the use of parametric identification techniques for modeling of biological systems.

The organization of this paper is as follows. The NARMAX model structure is described in Section II. In Section III a continuous-time representation of a parallel pathway model describing ankle dynamics is given, while its NARMAX representation is derived in Section IV. Section V illustrates the results of simulating this NARMAX representation of ankle dynamics. In Section VI a compressed NARMAX representation is derived to eliminate redundant parameters and Section VII assesses the applicability of NARMAX identification to this model representation via simulations of experimental conditions. Section VIII presents the results of identifying experimental human ankle data and Section IX provides a discussion of our major finds. Lastly, in Section X we give the conclusions and significance of our results.

II. NARMAX Model Description

The I/O relationship of many nonlinear dynamic systems can be written as the nonlinear difference equation

$$y(n) = F^l[y(n-1),\ldots,y(n-n_y),u(n),\ldots,u(n-n_u), e(n-1),\ldots,e(n-n_e)] + e(n) \quad (1)$$

where F^l is a nonlinear mapping, u is the "controlled" (i.e., exogenous) input, y is the output, and e is the innovation, or uncontrolled input. This structure describes both the stochastic and deterministic components of a system. This nonlinear mapping may include a variety of nonlinear terms, such as terms raised to an integer power [e.g., $u^2(n-3)$], products of present and past inputs [e.g., $u(n)u(n-1)$], past outputs [e.g., $y(n-1)y(n-2)$],

Manuscript received February 2, 2002; revised April 30, 2002. This work was supported by the Natural Sciences and Engineering Research Council of Canada, the Canadian Institutes of Health Research, and the Max Stein fellowships of McGill University. *Asterisk indicates corresponding author.*

S. L. Kukreja is with the Division of Automatic Control, Department of Electrical Engineering, Linköpings Universitet, SE-581 83 Linköping, Sweden.

H. L. Galiana is with the Department of Biomedical Engineering, McGill University, Montreal, QC H3A 2T5, Canada.

*R. E. Keraney is with the Department of Biomedical Engineering, McGill University, Montreal, QC H3A 2T5, Canada (e-mail: robert.kearney@mcgill.ca).

Digital Object Identifier 10.1109/TBME.2002.803507

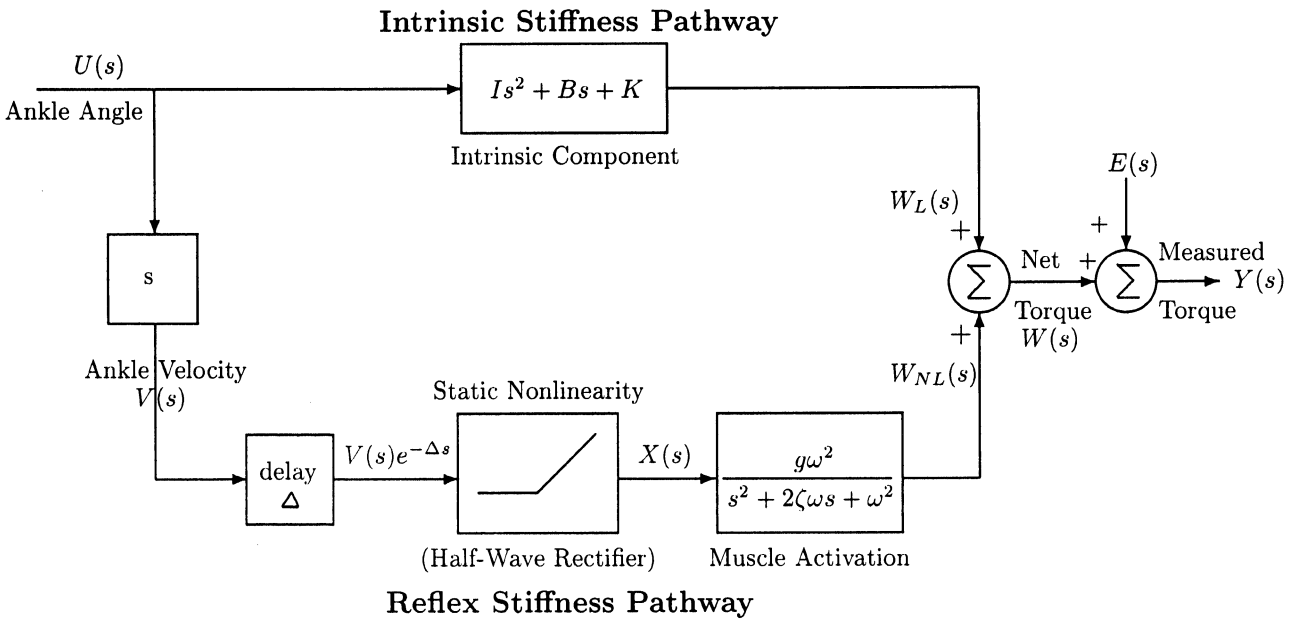

Fig. 1. System structure assumed for modeling and identification of intrinsic and reflex contributions to overall ankle torque.

or cross-terms [e.g., $u^2(n-1)y(n-2)$]. This system description encompasses most forms of nonlinear difference equations that are linear-in-the-parameters.

III. Parallel Pathway Model of Ankle Dynamics

Our laboratory, the Neuromuscular Control Laboratory, has developed a parallel pathway model (Fig. 1) to describe ankle dynamics [7]. This model treats the relationship between ankle angle and net ankle torque as the sum of a linear and nonlinear contributions. The upper, linear pathway models intrinsic stiffness as a second-order system with parameters corresponding to inertia (I), viscosity (B) and elasticity (K). The lower, nonlinear pathway models reflex stiffness as a cascade of a derivative, a time delay, a static nonlinearity (i.e., half-wave rectifier) defined as

$$x(t) = \begin{cases} 0, & v(t-\Delta) \le 0 \\ v(t-\Delta), & v(t-\Delta) > 0 \end{cases} \tag{2}$$

and a low-pass system representing muscle activation. The latter is simplified to second-order, though in many cases it has been shown to be better represented by a third-order filter [8], [9]. A second-order model is justified for the muscle activation since we assume that the "system" is a normal subject under passive conditions [8], [10]. The parameters associated with the low-pass system are damping parameter (ζ), natural frequency (ω) and gain (g).

A. Discrete-Domain Approximation to a Derivative Versus Bilinear Transform

The discrete-domain approximation to a derivative (Newton's backward formula) maps points from the left-half s plane into a circle of radius 1/2, centered at $z = 1/2$ in the z plane [11], [12]. Since this mapping confines the discrete-time poles to low frequencies, its use is restricted to systems with low resonant frequencies [12]. This is a good approximation to a derivative provided the bandlimit of interest is confined to low frequencies. For our work the bandlimit of interest is 0.15 of the sampling rate (see Section V); therefore, this approximation is appropriate for approximating the intrinsic component of ankle dynamics. Conversely, the bilinear transform maps the left-half s plane into the entire unit circle and, hence, does not have the same restrictions as above. The bilinear transform gives a better fit to the transient portion of a step response than does the discrete-domain approximation [11], [12]. For this reason, it is used to transform muscle activation dynamics, modeled as an infinitie impulse response (IIR) system, in Fig. 1.

However, in the finite impulse response case (intrinsic stiffness pathway Fig. 1) the bilinear transform cannot be used because, in general, it cannot transform an all-zero system into a stable discrete equivalent. (The bilinear transform is valid up to half the sampling rate, i.e., the Nyquist frequency.) Using the bilinear transform, a derivative operator in continuous-time transforms into a pole-zero system in discrete-time with a pole at $z = -1$. This discrete pole maps back to an unstable pole on the $j\omega$ axis in the s plane. For this reason, the derivative operator is transformed to discrete-time using Newton's backward formula [13].

IV. Theoretical Analysis

The parallel pathway model is given in continuous-time. In this section, we show how the model can be converted to discrete-time and rewritten as a NARMAX model. To do so, we note that the two pathways can be decoupled and analyzed separately since they are summed to yield the net torque.

The discrete-domain approximation to a derivative (Newton's backward formula [13])

$$s = \frac{d\,u(t)}{dt} \approx \frac{u(n) - u(n-1)}{T}$$
$$T \equiv \text{sampling rate}$$
$$n \equiv \text{sampled data point index} \tag{3}$$

was used to approximate the intrinsic pathway dynamics. In the nonlinear path the first derivative in the cascade was approximated using the same derivative approximation as in the linear path. The continuous-time delay was converted to discrete-time as

$$\tau = \left\lceil \frac{\Delta}{T} \right\rceil \tag{4}$$

where Δ is the continuous-time delay.

To compute a "theoretical" parameter set for this NARMAX model the half-wave rectifier, in the continuous-time model, was approximated, using a least-squares fit, as a second-order static polynomial ("DT Coefficients" in Table II)

$$c_0 + c_1 x(n) + c_2 x^2(n). \tag{5}$$

This second-order fit accounted for over 98% of the output variance of the static nonlinearity ("$X(s)$" in Fig. 1). The operating range of the velocity input ("$V(s)e^{-\Delta s}$") was between $\pm$30 rad/s and the position input ("$U(s)$") was between $\pm$0.40 rad. This range of input amplitude was selected to span a wide range of the nonlinearity and it is consistent with the amplitude range used for simulations (see Section V). A plot of this second-order approximation to the true half-wave rectifier is shown in Fig. 2.

The activation dynamics were converted to discrete-time via the bilinear transform

$$s = \frac{2}{T}\left(\frac{z-1}{z+1}\right). \tag{6}$$

In addition, we assumed the model was corrupted by output additive (measurement) noise as

$$y(n) = w(n) + e(n) \tag{7}$$

where $y(n)$ is the noise corrupted output, $w(n)$ the unmeasured noise free output and $e(n)$ the measurement noise.

After collecting terms and combining, the overall nonlinear model was represented as a nonlinear difference equation with 21 terms as [14]

$$\begin{aligned} y(n) =& b_0 + b_1 y(n-1) + b_2 y(n-2) + b_3 u(n) \\ &+ b_4 u(n-1) + b_5 u(n-2) + b_6 u(n-3) \\ &+ b_7 u(n-4) + b_8 u(n-\tau) + b_9 u(n-\tau-1) \\ &+ b_{10} u(n-\tau-2) + b_{11} u(n-\tau-3) \\ &+ b_{12} u^2(n-\tau) + b_{13} u^2(n-\tau-1) \\ &+ b_{14} u^2(n-\tau-2) + b_{15} u^2(n-\tau-3) \\ &+ b_{16} u(n-\tau) u(n-\tau-1) \\ &+ b_{17} u(n-\tau-1) u(n-\tau-2) \\ &+ b_{18} u(n-\tau-2) u(n-\tau-3) \\ &+ b_{19} e(n-1) + b_{20} e(n-2). \end{aligned} \tag{8}$$

This is a NARMAX model since 1) it includes I/O terms that are combinations of linear, nonlinear integer powers and cross-products and 2) is linear-in-the-parameters. Table I shows the relationship of discrete-time NARMAX parameters in (8) to the underlying continuous-time coefficients. Note that in this case many of the coefficients are related to each other. This will be addressed later (see Section VI).

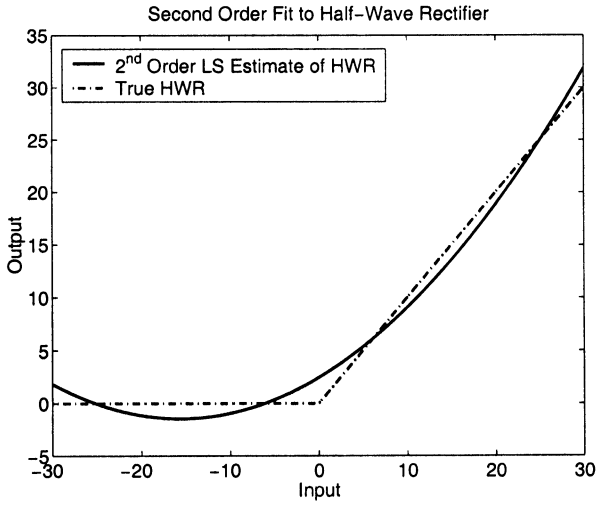

Fig. 2. Second-order least-squares approximation to the half-wave rectifier used in simulations.

V. Validation of NARMAX Ankle Model

The accuracy of this system representation was validated by simulating the parallel pathway model in continuous-time using Simulink (Fig. 1). The nonlinearity used in this continuous-time simulation was a "hard rectifier" (2); *not* the second-order power series simulated in continuous-time, e.g., (5). The parameters used in the simulation were typical values found in experiments ("CT Coefficients" and T in Table II) [7]. The system was excited using a 30-Hz band-limited, uniformly distributed, zero-mean, random input.

A. Output Accuracy

To determine the validity of this NARMAX description model (8) we simulated its response for a parameter set corresponding to that used for the continuous-time model. The input sequence was a band-limited, uniformly distributed, white, zero-mean, random input, low-pass filtered with an eighth-order 30-Hz Bessel filter. The band-limited input had an operating range between $\pm$0.40 rad (see upper panel of Fig. 3).

Assuming a second-order nonlinearity, the frequency content of the signal at the output of the half-wave rectifier ("$X(s)$" in Fig. 1) will be at least 60 Hz (twice the band-limited 30-Hz signal). To avoid internal aliasing, we selected a sampling rate of $T = 0.005$ s (200 Hz); 3.3 times greater than the internal 60 Hz signal.

The simulated output $(\hat{y}(n))$ of the NARMAX description model was compared with the output of the continuous-time simulation $(y(n))$ by computing the percent variance accounted for (%VAF) by the NARMAX model as

$$\%\text{VAF} = \left(1 - \frac{\frac{1}{N}\sum_{n=1}^{N} (y(n) - \hat{y}(n))^2}{\frac{1}{N}\sum_{n=1}^{N} (y(n))^2} \right) \times 100 \tag{9}$$

where N is the record length.

TABLE I
THEORETICAL RELATIONSHIP OF NARMAX PARAMETERS TO CONTINUOUS-TIME SYSTEM COEFFICIENTS FOR PARALLEL PATHWAY MODEL OF ANKLE DYNAMICS

NARMAX Coefficient	Linear Relationships	Relationship to Continuous-time Coefficient
b_0		$\frac{4c_0g\omega^2T^2}{4+\omega^2T^2+4\zeta\omega T}$
b_1		$-\frac{-8+2\omega^2T^2}{4+\omega^2T^2+4\zeta\omega T}$
b_2		$-\frac{-4\zeta\omega T+4+\omega^2T^2}{4+\omega^2T^2+4\zeta\omega T}$
b_3		$\frac{I}{T^2}+\frac{B}{T}+K$
b_4		$\frac{-2I}{T^2}-\frac{B}{T}-((-\frac{-8+2\omega^2T^2}{4+\omega^2T^2+4\zeta\omega T})(\frac{I}{T^2}+\frac{B}{T}+K))$
b_5		$\frac{I}{T^2}-((-\frac{-8+2\omega^2T^2}{4+\omega^2T^2+4\zeta\omega T})(\frac{-2I}{T^2}-\frac{B}{T}))$ $-((-\frac{-4\zeta\omega T+4+\omega^2T^2}{4+\omega^2T^2+4\zeta\omega T})(\frac{I}{T^2}+\frac{B}{T}+K))$
b_6		$-(-\frac{-8+2\omega^2T^2}{4+\omega^2T^2+4\zeta\omega T})(\frac{I}{T^2})-((-\frac{-4\zeta\omega T+4+\omega^2T^2}{4+\omega^2T^2+4\zeta\omega T})(\frac{-2I}{T^2}-\frac{B}{T}))$
b_7		$-((-\frac{-4\zeta\omega T+4+\omega^2T^2}{4+\omega^2T^2+4\zeta\omega T})\frac{I}{T^2})$
b_8	$b_8=b_9=-b_{10}=-b_{11}$	$\frac{g\omega^2T^2c_1}{(4+\omega^2T^2+4\zeta\omega T)T}$
b_9		$\frac{g\omega^2T^2c_1}{(4+\omega^2T^2+4\zeta\omega T)T}$
b_{10}		$\frac{-g\omega^2T^2c_1}{(4+\omega^2T^2+4\zeta\omega T)T}$
b_{11}		$\frac{-g\omega^2T^2c_1}{(4+\omega^2T^2+4\zeta\omega T)T}$
b_{12}		$\frac{g\omega^2T^2c_2}{(4+\omega^2T^2+4\zeta\omega T)T^2}$
b_{13}	$b_{13}=3b_{12}$	$\frac{3g\omega^2T^2c_2}{(4+\omega^2T^2+4\zeta\omega T)T^2}$
b_{14}	$b_{14}=3b_{12}$	$\frac{3g\omega^2T^2c_2}{(4+\omega^2T^2+4\zeta\omega T)T^2}$
b_{15}	$b_{15}=b_{12}$	$\frac{g\omega^2T^2c_2}{(4+\omega^2T^2+4\zeta\omega T)T^2}$
b_{16}	$b_{16}=-2b_{12}$	$\frac{-2g\omega^2T^2c_2}{(4+\omega^2T^2+4\zeta\omega T)T^2}$
b_{17}	$b_{17}=-4b_{12}$	$\frac{-4g\omega^2T^2c_2}{(4+\omega^2T^2+4\zeta\omega T)T^2}$
b_{18}	$b_{18}=-2b_{12}$	$\frac{-2g\omega^2T^2c_2}{(4+\omega^2T^2+4\zeta\omega T)T^2}$
b_{19}	$b_{19}=-b_1$	$\frac{-8+2\omega^2T^2}{4+\omega^2T^2+4\zeta\omega T}$
b_{20}	$b_{20}=-b_2$	$\frac{-4\zeta\omega T+4+\omega^2T^2}{4+\omega^2T^2+4\zeta\omega T}$

Fig. 3 shows the simulation input (upper panel) and predicted output of the NARMAX description model superimposed on top of the simulated output of the parallel pathway model (lower panel). With over 99%VAF the NARMAX output matched that of the continuous-time simulation with negligible error.

VI. REDUCTION OF DIMENSIONALITY

Identification of the full NARMAX representation given in (8) and Table I was shown to give highly biased estimates [15]. This bias might have been the result of several factors.

1) All prediction error identification (PEI) methods are only unbiased asymptotically.
2) The true values of NARMAX parameters are not accurate due to approximation or.
3) The relation between the parameters due to over-parameterization, i.e., correlation between some current NARMAX coefficients [16].

Explanation 1 is not reasonable since even with increased data length, the bias still remained [15]. In addition, explanation 2 is not reasonable since the NARMAX model (8) has been validated with a fit of 99%VAF. Hence, explanation 3 is the plausible reason for this bias.

Therefore, we investigated the effect of reducing the number of terms required to describe this NARMAX model. This is not a general reduction of terms to describe the data but rather a minimization of the number of regressors or degrees of freedom used to form the regressor matrix. This reduction should provide a regressor matrix that is more stable in terms of invertibility since the coefficients will no longer be interrelated [17].

The coefficients of the full NARMAX model ((8) and Table I) are partially redundant and, therefore, its I/O description can be redefined. Recombining all terms in (8) according to coefficients of the static nonlinearity (c_2, c_1 and c_0) yields an overall

TABLE II
UPPER: CONTINUOUS-TIME COEFFICIENT VALUES I: INERTIA, B: VISCOSITY, K: ELASTICITY, ω: NATURAL FREQUENCY, ζ: DAMPING PARAMETER, g: REFLEX STIFFNESS GAIN AND Δ: REFLEX DELAY. LOWER: COEFFICIENT VALUES OF STATIC NONLINEARITY. c_0: DC TERM, c_1: LINEAR TERM, c_2: SQUARED TERM AND T: SAMPLING INTERVAL

CT Coefficient	Value
I	0.015 Nm/s^2/rad
B	0.800 Nm/rad/s
K	150 Nm/rad
ω	40.0
ζ	1.00
g	10.00 Nm/rad/s
Δ	0.045 s
NL Coeff.	**Value**
c_0	2.46
c_1	0.500
c_2	0.016
T	0.005 s

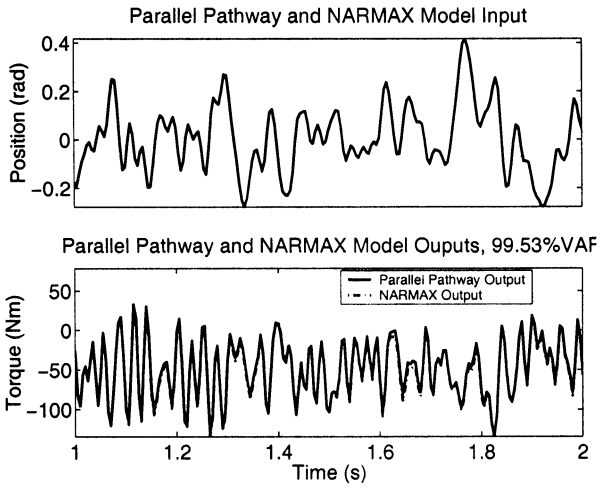

Fig. 3. (top) Input to simulated parallel pathway model in continuous-time and NARMAX description model. (bottom) Output of simulated parallel pathway model in continuous-time and NARMAX description model. Note that the two outputs are almost identical.

nonlinear model represented by 12 terms as

$$\begin{aligned} y(n) =& b_0 + b_1 y(n-1) + b_2 y(n-2) + b_3 u(n) \\ &+ b_4 u(n-1) + b_5 u(n-2) \\ &+ b_6 u(n-3) + b_7 u(n-4) \\ &+ m_1 \left[u(n-\tau) + u(n-\tau-1) \right. \\ &\qquad \left. -u(n-\tau-2) - u(n-\tau-3)\right] \\ &+ m_2 \left[u^2(n-\tau) + 3u^2(n-\tau-1) \right. \\ &\qquad + 3u^2(n-\tau-2) + u^2(n-\tau-3) \\ &\qquad - 2u(n-\tau)u(n-\tau-1) \\ &\qquad - 4u(n-\tau-1)u(n-\tau-2) \\ &\qquad \left. -2u(n-\tau-2)u(n-\tau-3)\right] \\ &+ b_{19} e(n-1) + b_{20} e(n-2) \\ =& b_0 + b_1 y(n-1) + b_2 y(n-2) + b_3 u(n) \\ &+ b_4 u(n-1) + b_5 u(n-2) + b_6 u(n-3) \\ &+ b_7 u(n-4) + m_1 \upsilon(n) + m_2 \chi(n) \\ &+ b_{19} e(n-1) + b_{20} e(n-2) \end{aligned} \tag{10}$$

where

$$\upsilon(n) = u(n-\tau) + u(n-\tau-1) - u(n-\tau-2) - u(n-\tau-3) \tag{11}$$

and

$$\begin{aligned} \chi(n) =& u^2(n-\tau) + 3u^2(n-\tau-1) + 3u^2(n-\tau-2) \\ &+ u^2(n-\tau-3) - 2u(n-\tau)u(n-\tau-1) \\ &- 4u(n-\tau-1)u(n-\tau-2) \\ &- 2u(n-\tau-2)u(n-\tau-3). \end{aligned} \tag{12}$$

Note that parameters b_1, b_{19} and b_2, b_{20} are not redefined because b_{19} and b_{20} are associated with noise and, therefore, are difficult to identify accurately (see Section VII-A). Consequently, any error estimating these parameters will affect the accuracy of redefined parameters as well.

Table III gives the relationships of these discrete-time NARMAX parameters (10) to the underlying continuous-time coefficients. This reduced set of coefficients now has the same number of degrees of freedom as the initial continuous-time description (the "extra" coefficient T denotes the sampling rate).

VII. IDENTIFICATION OF NARMAX ANKLE MODEL

We then assessed the utility of methods developed for identifying NARMAX models using sampled data from the continuous-time simulation. An extended least-squares (ELS) algorithm [2], [18] was used to identify model parameters.

The NARMAX description of the parallel pathway ankle model (10) is described by past outputs which are linear-in-the-parameters. In the presence of output additive noise (7), (8), these terms result in lagged values of disturbance terms which are also *linear-in-the-parameters* [19]. If these lagged errors are not modeled, they induce a bias in the parameter estimates [2], [18]–[20]. The ELS algorithm was implemented because it is designed to model lagged error terms thereby providing unbiased parameter estimates.

It is well known that ELS suffers from convergence problems [16], [20], [21]. However, no PEI method is optimal. For the ankle model, we deem that this is the best estimation technique because it provides an unbiased estimate of model parameters [20]. Other estimation techniques such as maximum-likelihood, instrumental variables, weighted least-squares, etc., are difficult to implement and also have convergence problems [20]–[22]. For this reason, we chose to use ELS.

For this study, the system order and structure were assumed to be known with the reduced coefficient set in (10) and Table III. The regressor matrix used by this algorithm was formed to contain only those columns (parameters) that corresponded to our theoretical analysis (10). It is reasonable to assume that the order and structure are known because our goal is to identify a model in the model class described by (10). The estimation set consisted of $N = 4000$ data points sampled at $T = 0.005$ s. The estimated parameters were cross-validated to compute the

TABLE III
THEORETICAL RELATIONSHIP OF COMPRESSED NARMAX MODEL PARAMETER SET TO CONTINUOUS-TIME SYSTEM COEFFICIENTS

NARMAX Coefficient	Relationship to Continuous-time Coefficient
b_0	$\frac{4c_0 g\omega^2 T^2}{4+\omega^2T^2+4\zeta\omega T}$
b_1	$-\frac{-8+2\omega^2T^2}{4+\omega^2T^2+4\zeta\omega T}$
b_2	$-\frac{-4\zeta\omega T+4+\omega^2T^2}{4+\omega^2T^2+4\zeta\omega T}$
b_3	$\frac{I}{T^2}+\frac{B}{T}+K$
b_4	$\frac{-2I}{T^2}-\frac{B}{T}-((-\frac{-8+2\omega^2T^2}{4+\omega^2T^2+4\zeta\omega T})(\frac{I}{T^2}+\frac{B}{T}+K))$
b_5	$\frac{I}{T^2}-((-\frac{-8+2\omega^2T^2}{4+\omega^2T^2+4\zeta\omega T})(\frac{-2I}{T^2}-\frac{B}{T}))-((-\frac{-4\zeta\omega T+4+\omega^2T^2}{4+\omega^2T^2+4\zeta\omega T})(\frac{I}{T^2}+\frac{B}{T}+K))$
b_6	$-(-\frac{-8+2\omega^2T^2}{4+\omega^2T^2+4\zeta\omega T})(\frac{I}{T^2})-((-\frac{-4\zeta\omega T+4+\omega^2T^2}{4+\omega^2T^2+4\zeta\omega T})(\frac{-2I}{T^2}-\frac{B}{T}))$
b_7	$-((-\frac{-4\zeta\omega T+4+\omega^2T^2}{4+\omega^2T^2+4\zeta\omega T})\frac{I}{T^2})$
m_1	$\frac{g\omega^2T^2c_1}{(4+\omega^2T^2+4\zeta\omega T)T}$
m_2	$\frac{g\omega^2T^2c_2}{(4+\omega^2T^2+4\zeta\omega T)T^2}$
b_{19}	$\frac{-8+2\omega^2T^2}{4+\omega^2T^2+4\zeta\omega T}$
b_{20}	$\frac{-4\zeta\omega T+4+\omega^2T^2}{4+\omega^2T^2+4\zeta\omega T}$

%VAF of the net predicted torque. The validation set consisted of $N_v = 2000$ data points [20], [23].

A. Analysis of Compressed NARMAX Model Parameters

A Monte Carlo study of these reduced NARMAX parameters [(10), Table III] was performed to assess their accuracy and variability. Fig. 4 shows the results of this study. The NARMAX parameters in this figure correspond to those given in Table III. Parameters m_1 and m_2 in Fig. 4 correspond to parameters b_8–b_{11} and b_{12}–b_{18} in Table I. This figure shows that, when the number of terms describing this NARMAX model was reduced to the appropriate complexity, the identified parameter values corresponded closely to those derived theoretically for signal-to-noise ratios (SNRs) $\geq$20 dB. Note that we do not expect the mean value of parameters b_{19} and b_{20} to be close to the theoretically computed value since they correspond to lagged error terms. Lagged error terms are difficult to identify accurately even with high SNR since they model the output additive noise which is a stochastic process and cannot be measured. This stochastic process is modeled (approximated) by a deterministic signal of prediction errors which is only a (poor) estimate of the noise [18], [20].

Fig. 5 shows a predicted output superimposed on top of the measured output for a typical parameter set using cross-validation data. The predicted output matched the measured output with over 98%VAF.

B. Analysis of Input Noise Sensitivity

In the preceding section we only examined the effects of output noise on NARMAX parameters of ankle dynamics. It is well known that standard least-squares was not developed to tolerate input noise [24]–[27]. When studying ankle dynamics, under experimental conditions, it is known that the input may not be measured with negligible error. In our laboratory, experimental [pseudorandom binary sequence (PRBS)] inputs [7] are typically in the range of 0.005–0.2 rad. The convention used in the laboratory is 0.1 rad = 1 V. The I/O is recorded with a 16-bit analog-to-digital (A/D) (IOTech ADC488) and has a 20-V dynamic range. The input SNR is computed as [12, p. 756]

$$\begin{aligned}\mathrm{SNR}\,db &= 10\log_{10}\frac{P_x}{P_n} = 10\log_{10}\left(\frac{2\sqrt{12}\sigma_x 2^b}{R}\right)^2\\ &= 20\log_{10}2\sqrt{12} + b20\log_{10}2 - 20\log_{10}\frac{R}{\sigma_x}\\ &\approx 16.81 + 6.02b - 20\log_{10}\left(\frac{R}{\sigma_x}\right)\end{aligned} \tag{13}$$

where

R	range of quantizer;
b	number of bits;
$\gamma = (R/2^{b+1})$	quantization step size;
$P_n = (\gamma^2/12)$	noise variance;
$P_x = \sigma_x^2$	signal variance.

This yields an input SNR (assuming no other input noise source) approximately in the range of 108 dB–76 dB. Although this corresponds to small amplitude noise, we examined the effects of input noise on our ELS parameter estimation algorithm.

For this study, simulation and estimation protocols remained the same as described in Section VII except that a PRBS input was used to excite the system dynamics, since it is standard practice in our laboratory. Note that this PRBS input is very non-Gaussian and nonwhite [1]. A switch of input in this study may cause concern since it may change sensitivity to output noise for our estimation technique. This is not true for linear regression problems which are solved by least-squares methods,as long as the input signal is persistently exciting, i.e., that the system dy-

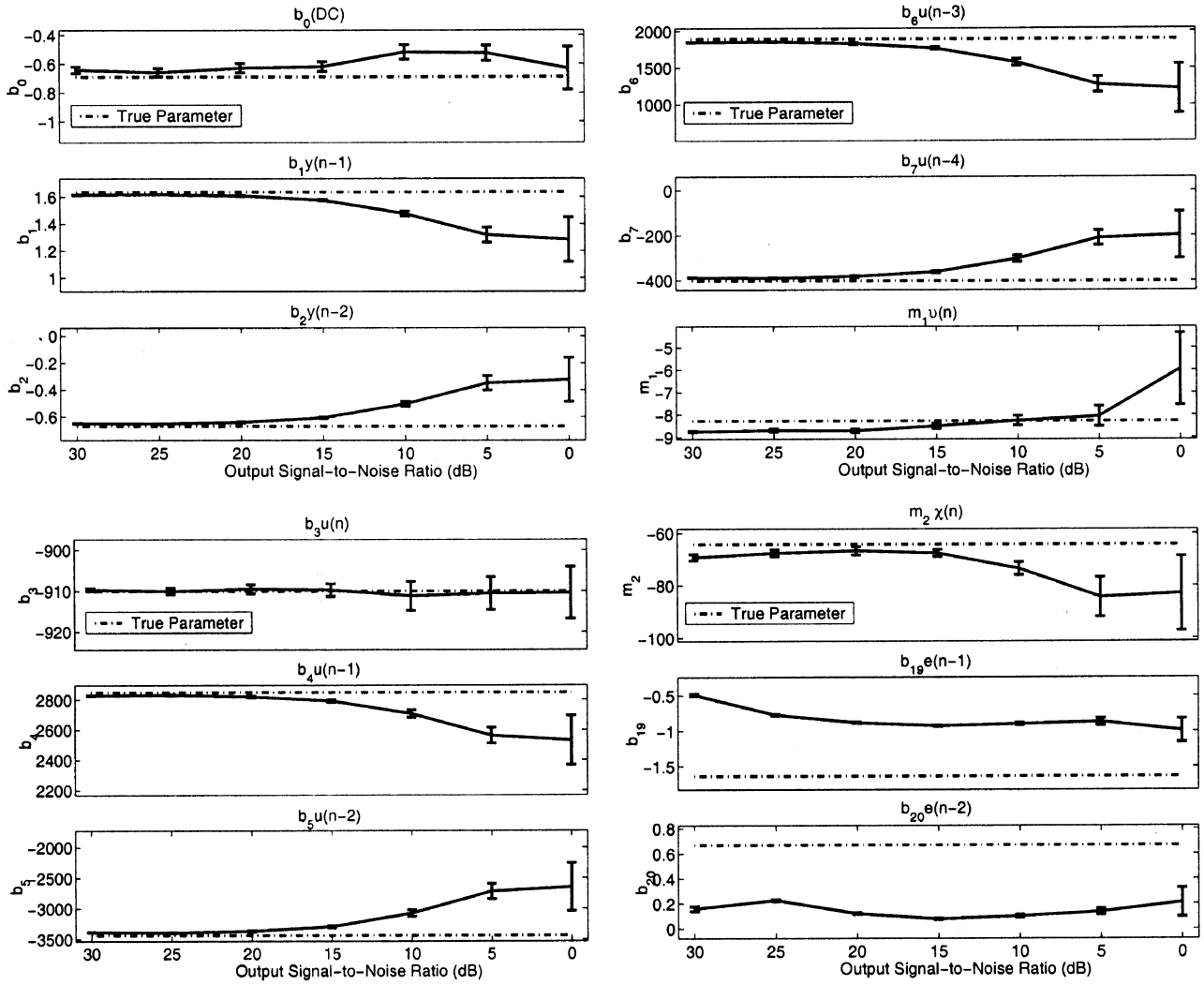

Fig. 4. Compressed NARMAX model: Bandlimited, zero-mean, random input, Gaussian, white, zero-mean noise, and $N = 4000$. Ordinate: STD about mean. Abscissa: Output $\mathrm{SNR} = 20$, 25, 20, 15, 10, 5, and 0 dB. (Note that the abscissa is shown in decreasing SNR which corresponds to increasing noise intensity.).

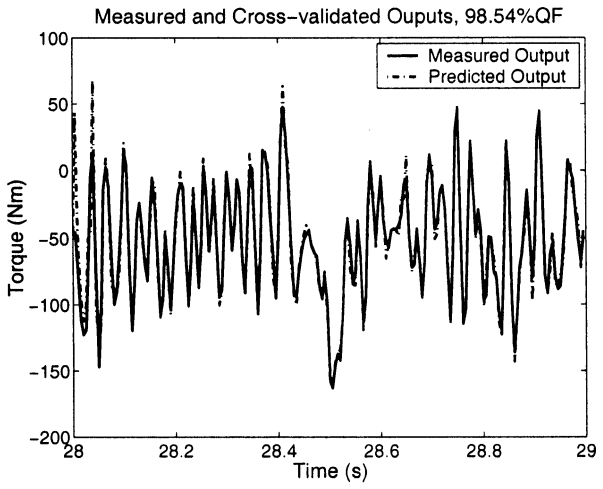

Fig. 5. Cross-validation: Measured and predicted output for identified NARMAX ankle model with $N_v = 2000$ and Gaussian, white, zero-mean output additive noise (20-dB SNR).

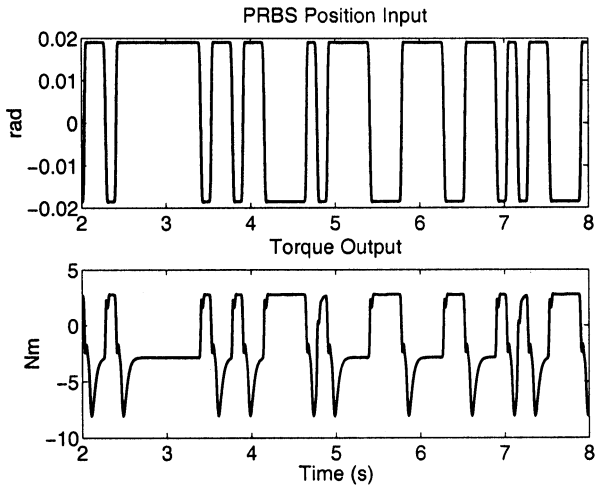

Fig. 6. Typical position input and torque output recorded from a simulation used to assess input noise sensitivity.

namics be persistently excited over the measurement time [20]. A PRBS input has been shown to be a sufficiently exciting input for the identification of ankle dynamics [7].

Fig. 6 shows a typical I/O trial used for this analysis. The data represents a PRBS sequence of 0.0375 rad (peak-to-peak) and

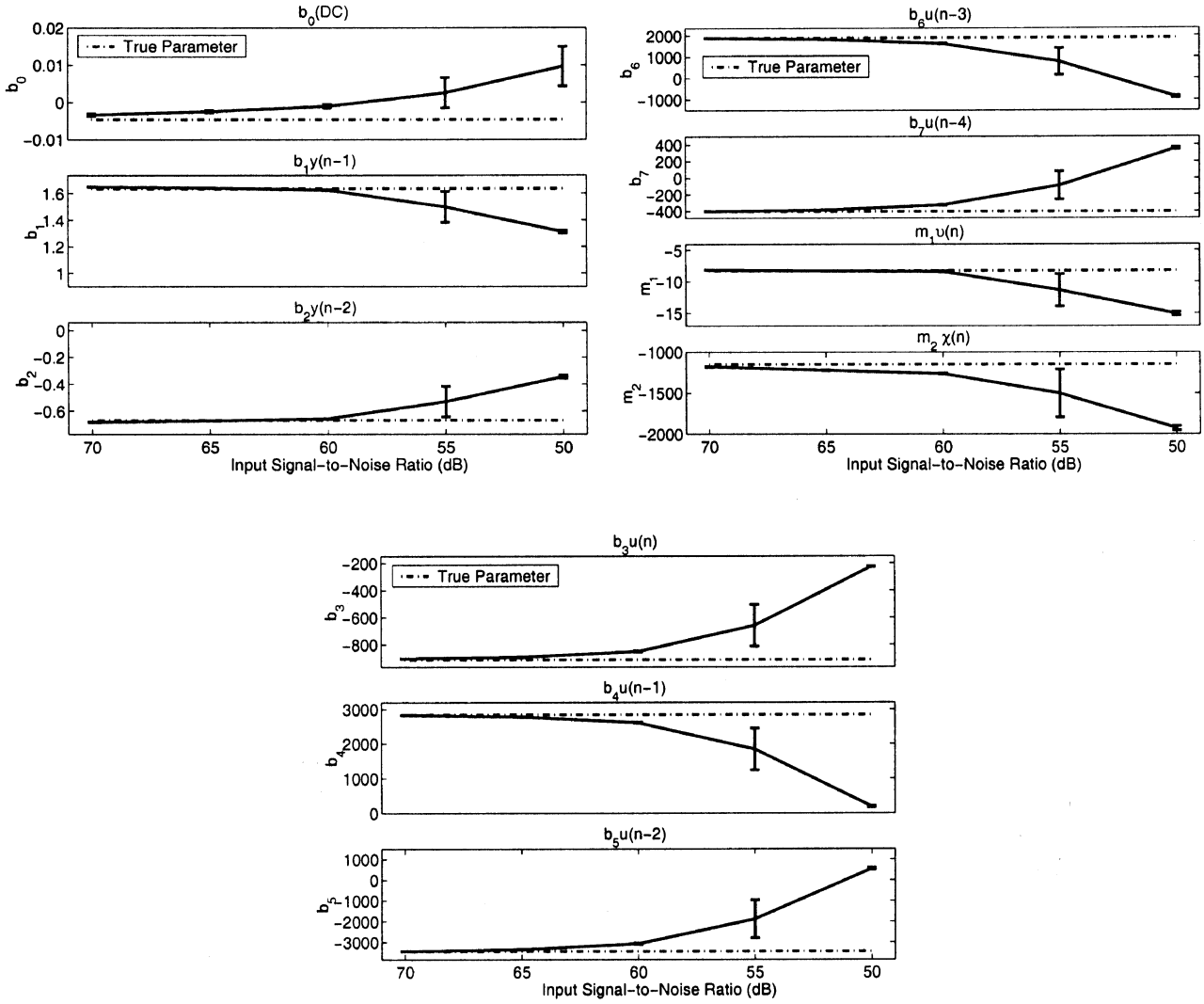

Fig. 7. Compressed NARMAX model: PRBS input, Gaussian, white, zero-mean input noise and $N = 7000$. Ordinate: STD about mean. Abscissa: Input $\mathrm{SNR} = 70, 65, 60, 55$, and 50 dB. Dashed line: True parameter value. (Note that the abscissa is shown in decreasing SNR which corresponds to increasing noise intensity.).

125-ms switching rate. The characteristics of this trial are consistent with those used for analysis in this section. A unique, Gaussian, white, zero-mean noise sequence was added to the input, noise amplitude was increased in increments of 5 dB, from 70-dB to 50-dB SNR, the output was noise-free, and $N = 7000$ data points were used for estimation.

The results of this study are summarized in Fig. 7 and correspond to the reduced NARMAX model (Section X & Table III). These plots show that even when an insignificant amount of input noise was added (with noise-free output) NARMAX parameters deviated significantly from their true values. Note that parameters b_0 and b_4–b_7, associated with input only, flipped signs for SNR levels $\leq$55 dB SNR and, therefore, cannot be distinguished from zero. This bias may be the combination of two factors: 1) violation of least-squares theory and/or 2) model representation, i.e., high-pass nature of the linear path.

C. Analysis of Input and Output Noise Sensitivity

Although the previous study showed that even an insignificant amount of noise on the input yields highly biased parameters, we investigated the sensitivity of this identification approach to both input and output noise. This study was conducted to assess the likely performance of our algorithm under true experimental conditions.

Simulation and estimation protocols remained the same as described in Section VII-B. The input and output noise sequences were unique, Gaussian, white, zero-mean processes which were uncorrelated with the input and each other. The input noise sequence was fixed to have a SNR of 60 dB while the output additive noise amplitude was increased in increments of 5 dB, from 30 dB to 0 dB.

Results of this study are summarized in Fig. 8. These parameters correspond to NARMAX parameters given in Table III. The plots in this figure show that, for input SNR of 60 dB, some NARMAX parameters deviated significantly from their true values for output $\mathrm{SNR} \leq 10$ dB (see parameters b_1, b_2, b_4, b_7 and b_{20}). This bias is likely due to input additive noise, since our technique performs well with only output additive noise (see Section VII-A). This result is expected if the estimation technique used is ELS, and it implies the need to apply total least-squares (TLS) for these experimental conditions.

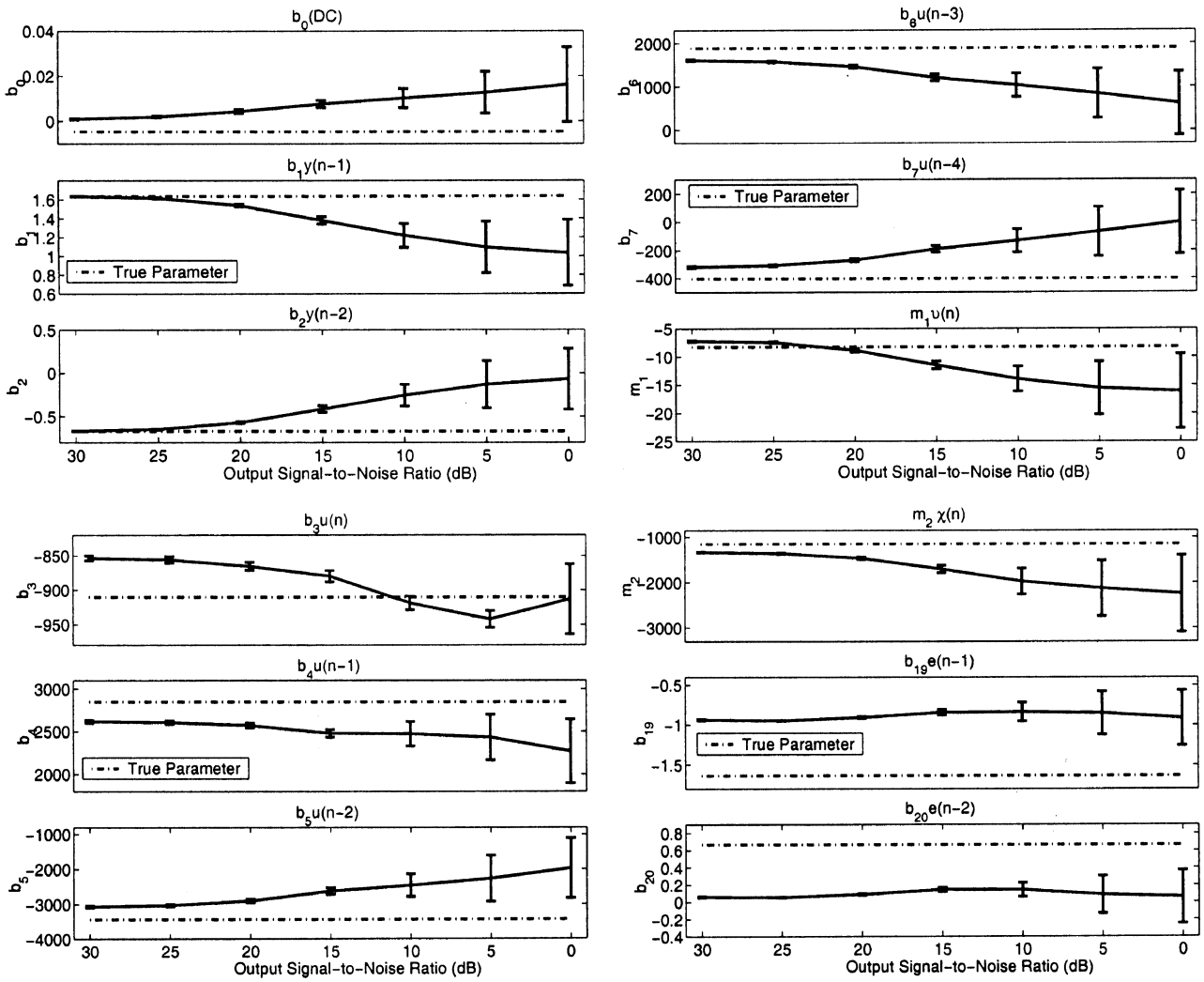

Fig. 8. Compressed NARMAX model: PRBS input, Gaussian, white, zero-mean input and output noise and $N = 7000$. Input $\mathrm{SNR} = 60$ dB. Ordinate: STD about mean. Abscissa: Output $\mathrm{SNR} = 30, 25, 20, 15, 10, 5$, and 0dB. (Note that the abscissa is shown in decreasing SNR which corresponds to increasing noise intensity.)

VIII. Experimental Data

Lastly, we assessed our identification technique on experimental human ankle data collected in our laboratory. The data analyzed for this study is from a single subject with no history of neuromuscular disease.

A. Apparatus

The subject lay supine with his foot attached to the pedal of an actuator by a custom fitted fiberglass boot [28], [29]. The fiberglass boot was firm enough to prevent heel movement during experiments without excessively restricting range of ankle rotation. Sandbags and a kneestrap held the knee fully extended.

An electro-hydraulic actuator operated as a position-servo driving the ankle position to follow a command input with a bandwidth of 0–80 Hz. Ankle position was measured with a precision potentiometer (Beckman 6273-R5K) while torque was recorded using a torque transducer (Lebow 2110–5 K) mounted in series with the subject's ankle [28].

An angle of 90° between the shank and foot was considered as the neutral position and defined as zero. Displacements in the dorsiflexing direction were considered as positive and those in the plantarflexing direction as negative. Torque was assigned a polarity consistent with the direction of movement [28].

B. Perturbations

PRBS inputs were used to excite the dynamics of this system. Data records in which input sequences had a peak-to-peak amplitude of 0.01–0.05 rad and a switching rate of 45–260 ms were used for this study.

C. Procedures

The subject was instructed to maintain a constant level of activation and not to resist the perturbations. Torque generated by the subject was measured, low-pass filtered, and fed back to an oscilloscope mounted above the subject's head. The subject was asked to match the torque feedback to a command signal displayed on the oscilloscope. Each PRBS sequence was started once the subject matched the desired torque level and recording was initiated after the subject re-established a stable contraction at the desired level [28]. The measured data was anti-alias fil-

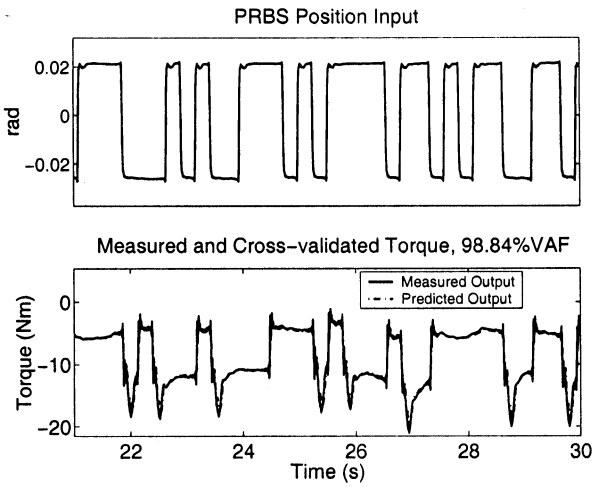

Fig. 9. Typical position input and torque output. (lower panel) Cross-validation. Predicted output superimposed on records measured output for identified NARMAX ankle model for experimental data set with $N_v = 1000$.

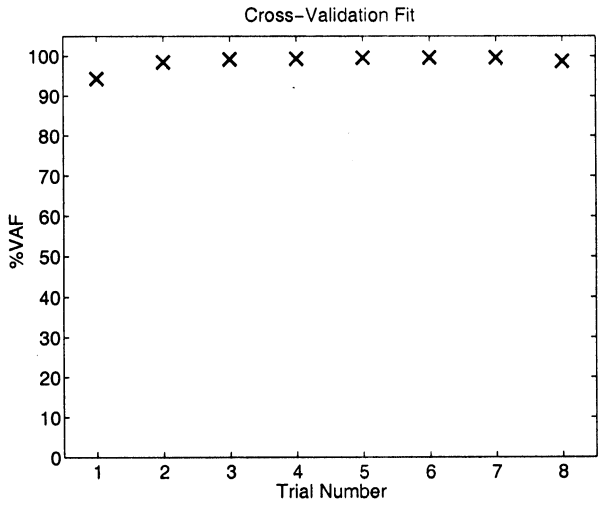

Fig. 10. Cross-validation. %VAF versus experimental trial.

tered with an eighth-order 200 Hz Bessel filter (Frequency Devices, 64 PF) and sampled at 1000 Hz by a 16-bit A/D converter (IOTech ADC488). Each I/O set was recorded for 30 s.

After recording, the experimental data was decimated by a factor of ten, resulting in a final sampling rate of 100 Hz. The system (ankle dynamics) was identified using our NARMAX approach, as outlined in Section VII, except that $N = 2000$ points was used for estimation and $N_v = 1000$ points was used for validation. Our least-squares algorithm fitted parameters for the model with a fixed delay and repeated the estimation with delays ranging from 50 to 100 ms. The parameter set and delay which yielded the highest cross-validation %VAF was deemed the best-fit model.

D. Results

The results of identifying eight trials of human ankle experiments are presented. Fig. 9 shows a typical I/O trial used for this analysis. The data represents a PRBS sequence of 0.05 rad and 260-ms switching rate while the subject maintained a mean contraction of −5 Nm. The characteristics of this trial are consistent with those reported in previous work from our laboratory [28]. The lower panel of Fig. 9 displays the cross-validation (predicted) output superimposed on the measured output, for this trial. The predicted output matched the measured output with over 98%VAF.

Fig. 10 shows the cross-validation %VAF for each trial. The results show that the predicted output, for these parameter estimates, account for a large portion of the variance. The %VAF ranged from a minimum of 94.43% to a maximum of 99.64%. For the eight trials examined for this study, 62.50% of predicted outputs accounted for more than 99%VAF of the measured output. This indicates that the NARMAX parameters explain the I/O data well. For the remaining 37.5% of the cases, the %VAF of predicted outputs range from 98.50%VAF to 94.43%VAF. Although these fits have a lower %VAF, they still indicate the NARMAX parameters explain the I/O data well.

IX. Discussion

A. NARMAX Representation of Ankle Dynamics

The theoretical results demonstrate that the nonlinear difference equation description for the parallel pathway model is a NARMAX model. Simulation results show that the NARMAX model matches the continuous-time response well. This suggests that parametric nonlinear model forms such as the NARMAX class can be used for modeling biological systems.

This discrete model provides excellent predictions, but it is not easy to map its parameters back into continuous-time coefficients due to instability of the mapping which is related to sampling rate and possibly incorrect inter-sample assumptions, i.e., zero-order hold [15]. This does not mean that the results in discrete form would not be useful. Statistical studies of NARMAX coefficients could be of direct clinical relevance for diagnosis, without mapping into their continuous-time forms. However, using these estimates for diagnosis requires care since different discretization methods will give different parameter values but should not lead to different diagnosis. This remains to be tested by examining the discrete parameter for different patient/normal populations.

B. Discrete-Time Parameter Estimation of Simulated Ankle Model

Simulation studies in Section VI showed that, for a compressed NARMAX model representation, the mean of Monte Carlo estimates for NARMAX parameters representing the linear dynamic components matched the theoretical values well for high SNR. However, estimates of some nonlinear parameters, e.g., m_1, did not correspond well to theoretically computed values. This bias may be a result of using a low-order approximation to the half-wave rectifier. A stiff nonlinearity of this form is of high order and, therefore, a second-order fit is only an approximation. The mean value of the NARMAX identified parameters may therefore give a better estimate of the system coefficients.

Currently, in our laboratory a nonparametric identification technique is used to estimate parameters describing ankle dynamics [1], [7], [30]–[33]. This nonparametric method

implements a Levenberg-Marquardt nonlinear least-squares algorithm which is iterative and requires an initial "guess" of the unknown model parameters to compute them [7]. In contrast, our nonlinear parametric approach permits one-step estimation of model parameters and does not require any initial guess.

C. Experimental Data

High %VAF cross-validation fits obtained for parameter estimates using NARMAX identification methods (see Fig. 10) show that the identified parameters explain the I/O data well. Using %VAF alone as an indicator of model goodness may lead to incorrect interpretations of model validity. However, in many cases, for nonlinear models, this may be the only indicator that is readily available.

A model validation technique for nonlinear systems, using higher-order correlations, was developed by Billings and Voon [34], [35]. Korenberg and Hunter [36] showed that this model validation technique fails for simple cases. Therefore, we did not implement this approach and used the %VAF alone as an indicator of model goodness.

When studying biological systems it may not be practical to assume that the exact model order and structure are well known *a priori*. In physiological systems analysis one of the main objectives is not only to estimate system parameters but to gain insight into the structure of the underlying system. It would be worthwhile in a future study to investigate what happens if NARMAX structure detection methods [19], [37]–[41] are allowed to free run on the data to find the best structure from the data set. This may then indicate deficiencies in the analytical model and could lead to improved modeling strategies.

X. Conclusions

Theoretical results demonstrate that the nonlinear difference equation description for the parallel pathway model of ankle dynamics is a NARMAX model. Simulation results show that the NARMAX model matches the continuous-time response well. Mapping of differential forms into NARMAX forms will usually result in more discrete parameters than there are degrees of freedom. It is important to recombine regressor matrix columns to obtain the appropriate dimension in free parameters. Failure to do so will lead to biased results. Moreover, this paper contributes to the understanding of the use of parametric identification techniques for modeling of biological systems.

We have demonstrated the importance of considering input noise sensitivity when implementing standard least-squares methods for analyzing experimental data. Therefore, unless the input is recorded with high precision or a noise-free record is available, it may be advantageous to consider alternative estimation methods such as TLS. These noise issues remain to be explored in detail but are manageable. The main point here is that the NARMAX form is clearly amenable to the study of a wide range of biological systems, and could be computationally efficient. It should be examined further especially in the case of severe nonlinear behavior.

Acknowledgment

The authors would like to dedicated this work in loving memory of Margherita Rapagna (August 25, 1968–May 20, 2002).

References

[1] R. E. Kearney and I. W. Hunter, "System identification of human joint dynamics," *Crit. Rev. Biomed. Eng.*, vol. 18, no. 1, pp. 55–87, 1990.
[2] S. A. Billings and W. S. F. Voon, "Least squares parameter estimation algorithms for nonlinear systems," *Int. J. Syst. Sci.*, vol. 15, no. 6, pp. 601–615, 1984.
[3] I. J. Leontaritis and S. A. Billings, "Input–output parametric models for nonlinear systems part I: Deterministic nonlinear systems," *Int. J. Contr.*, vol. 41, no. 2, pp. 303–328, 1985.
[4] ——, "Input–output parametric models for nonlinear systems part II: Stochastic nonlinear systems," *Int. J. Contr.*, vol. 41, no. 2, pp. 329–344, 1985.
[5] S. A. Billings and S. Chen, "Extended model set, global data and threshold model identification of severely nonlinear systems," *Int. J. Contr.*, vol. 50, no. 5, pp. 1897–1923, 1989.
[6] S. Chen and S. A. Billings, "Representations of nonlinear systems: The NARMAX model," *Int. J. Contr.*, vol. 49, no. 3, pp. 1013–1032, 1989.
[7] R. E. Kearney, R. B. Stein, and L. Parameswaian, "Identification of intrinsic and reflex contributions to human ankle stiffness dynamics," *IEEE Trans. Biomed. Eng.*, vol. 44, pp. 493–504, Juna 1997.
[8] M. M. Mirbagheri and R. E. Kearney, "Mechanisms underlying a third-order parametric model of dynamic reflex stiffness," in *Proc. IEEE EMBS*, vol. 22, Chicago, IL, July 2000, pp. 1241–1242.
[9] M. M. Mirbagheri, R. E. Kearney, H. Barbeau, and M. Ladouceur, "Parametric modeling of the reflex contribution to dynamic ankle stiffness in normal and spinal cord injured spastic subjects," in *Proc. IEEE EMBS*, vol. 17, Montreal, Canada, Sept. 1995, pp. 1241–1242.
[10] M. M. Mirbagheri, H. Barbeau, N. Ladouceur, and R. E. Kearney, "Intrinsic and reflex stiffness in normal and spastic spinal cord injured subjects," *Exp. Brain Res.*, vol. 141, pp. 446–459, 2001.
[11] S. S. Haykin, "A unified treatment of recursive digital filtering," *IEEE Trans. Automat. Contr.*, vol. AC-17, pp. 113–116, 1972.
[12] J. G. Proakis and D. G. Manolakis, *Digital Signal Processing: Principles, Algorithms, and Applications*, third ed. Englewood Cliffs, NJ: Prentice Hall, 1996.
[13] K. J. Åström, *Computer-Controlled Systems: Theory and Design*, 3rd ed. Upper Saddle River, N.J.: Prentice Hall, 1997.
[14] S. L. Kukreja, R. Kearney, and H. L. Galiana, "NARMAX representation of a parallel pathway model of ankle dynamics," in *Proc. CMBEC*, vol. 24, Edmonton, AB, Canada, June 1998, pp. 30–31.
[15] S. L. Kukreja, "Parametric Methods for Nonlinear System Identification," Ph.D. dissertation, Dept. Biomed. Eng., McGill Univ., Montreal, QC, Canada, 2001.
[16] É. Walter and L. Pronzato, *Identification of Parametric Models*, 1st ed. Berlin, Germany: Springer-Verlag, 1997.
[17] G. Golub, *Matrix Computation*, 2nd ed. Baltimore, MD: The Johns Hopkins Univ. Press, 1993.
[18] G. C. Goodwin and R. L. Payne, *Dynamic System Identification: Experiment Design and Data Analysis*. New York: Academic, 1977, vol. 136, Mathematics in Science and Engineering.
[19] S. L. Kukreja, H. L. Galiana, and R. E. Kearney, "A bootstrap method for structure detection of NARMAX models," Int. J. Contr., Dec. 2001, submitted for publication.
[20] L. Ljung, *System Identification: Theory for the User*, 2nd ed. Englewood Cliffs, NJ: Prentice-Hall, 1999.
[21] T. Shderstrbm and P. Stoica, *System Identification*. Englewood Cliffs, NJ: Prentice-Hall, 1989.
[22] P. Stoica and T. Sbderstrhm, "Asymptotic behavior of some bootstrap estimators," *Mt. J. Contr.*, vol. 33, no. 3, pp. 433–454, 1981.
[23] J. Shao, "Linear model selection by cross-validation," *J. Amer. Statist. Assoc.*, vol. 88, pp. 486–494, 1993.
[24] N. R. Draper and H. Smith, *Applied Regression Analysis*, 2nd ed. New York: Wiley, 1981.
[25] J. M. Mendel, *Lessons in Estimation Theory for Signal Processing, Communications and Control*, first ed. Englewood Cliffs, NJ: Prentice Hall, 1995.
[26] C. W. Ostrom, *Time Series Analysis: Regression Techniques*, 2nd ed. Newberry Park, CA: Sage, 1990.

[27] G. A. F. Seber, *Linear Regression Analysis*, 1st ed. New York: Wiley, 1977.
[28] M. M. Mirbagheri, H. Barbeau, and R. E. Kearney, "Intrinsic and reflex contributions to human ankle stiffness: Variation with activation level and position," *Exp. Brain Res.*, vol. 135, pp. 423–436, 2000.
[29] R. L. Morier, P .L. Weiss, and R. E. Kearney, "Low inertia, rigid limb fixation using glass fiber casting bandage," *Med. Biol. Eng. Comput.*, vol. 28, pp. 96–99, 1990.
[30] I. W. Hunter and R. E. Kearney, "Dynamics of human ankle stifness: Variation with mean ankle torque," *J. Biomech.*, vol. 15, no. 3, pp. 753–756, 1982.
[31] R. E. Kearney and I. W. Hunter, "System identification of human triceps surae stretch reflex dynamics," *Exp. Brain Res.*, vol. 51, pp. 117–127, 1983.
[32] ——, "Nonlinear identification of stretch reflex dynamics," *Ann. Biomed. Eng.*, vol. 16, pp. 79–94, 1988.
[33] R. E. Kearney, P. L. Weiss, and R. Morier, "System identification of human ankle dynamics: Intersubject variability and intrasubject reliability," *Clin. Biomech.*, vol. 5, no. 4, pp. 205–217, 1990.
[34] S. A. Billings and W. S. F. Voon, "Structure detection and model validation tests in the identification of nonlinear systems," *Inst. Elect. Eng. Proc.*, pt. D, vol. 130, pp. 193–199, 1983.
[35] ——, "Correlation based model validity tests for nonlinear models," *Int. J. Contr.*, vol. 44, no. 1, pp. 235–244, 1986.
[36] M. J. Korenberg and I. W. Hunter, "The identification of nonlinear biological systems: Wiener kernel approaches," *Ann. Biomed. Eng.*, vol. 8, pp. 629–654, 1990.
[37] M. J. Korenberg, "Orthogonal identification of nonlinear difference equation models," in *Proc. Midwest Symp. Circuit Theory*, vol. 1, 1985, pp. 90–95.
[38] M. J. Korenberg, S. A. Billings, Y. P. Liu, and P. J. McIlroy, "Orthogonal parameter estimation algorithm for nonlinear stochastic systems," *Int. J. Contr.*, vol. 48, no. 1, pp. 193–210, 1988.
[39] S. L. Kukreja, H. L. Galiana, and R. Kearney, "Structure detection of NARMAX models using bootstrap methods," in *Proc. 38th IEEE Conf. Decision and Control*, vol. 38, Phoenix, AZ, Dec. 1999, pp. 1071–1076.
[40] S. L. Kukreja, R. E. Kearney, and H. L. Galiana, "A bootstrap method for NARMAX model order selection," in *Proc. 4th IFAC Symp. Modeling and Control in Biomedical Systems*, vol. 4, Karlsburg/Greifswald, Germany, Mar. 2000, pp. 353–356.
[41] ——, "Structure detection of nonlinear dynamic systems using bootstrap methods," in *Proc. IEEE EMBS*, vol. 20, Hong Kong, China, Oct. 1998, pp. 3020–3023.

Sunil L. Kukreja was born in Baroda, India. He received the B.S. degree in electrical engineering from Johns Hopkins University, Baltimore, MD, in 1993. He received the M.Eng. and Ph.D. degrees in biomedical engineering from McGill University, Montreal, QC, Canada, in 1997 and 2001, respectively.

Since 2001, he has been a Post-Doctoral Fellow with the Division of Automatic Control, Department of Electrical Engineering, Linköping Universitet, Linköping, Sweden. His current research interest include algorithmic development for nonlinear switched (hybrid) systems, multiple internal state Wiener systems, continuous-discrete-continuous mappings, structure computation, order estimation, identification for biology, and uncertainty modeling for robust control.

Henrietta L. Galiana (M'87–SM'93–F'02) received the B.S. degree in electrical engineering (honors) and the M.E.E degree (biomedical) from McGill University, Montreal, QC, Canada, in 1966 and 1968, respectively. After a few years working with L. Young at the Man-Vehicle Laboratory, Massachusetts Institutes of Technology (MIT), Cambridge, and a seven-year sabbatical to raise two children, she returned to doctoral studies and received the Ph.D. degree in biomedical engineering from McGill University, in 1981.

Following a Post-Doc position at McGill's Aerospace Medical Research Unit, with G. Melvill Jones, she was offered a staff position in the new Department of Biomedical Engineering, where she now holds the position of Full Professor. Her research interests focus on signal processing and the modeling of control strategies for the orientation of eyes and head, and related issues of platform coordination and sensory fusion. Theoretical predictions are tested in a vestibular clinic for patient evaluation, and by porting controls to biomimetic systems.

She is an IEEE Fellow and is the current President (2002) of the Engineering in Medicine and Biology Society.

Robert E. Kearney (M'76–SM'92–F'01) received the Ph.D. degree in mechanical engineering from McGill University, Montreal, QC, Canada, in 1976.

He is a Professor and Chair of the Department of Biomedical Engineering at McGill University. He maintains an active research program that focuses on using quantitative engineering techniques to address important biomedical problems. His specific areas of research include: The development of algorithms and tools for biomedical system identification; the application of system identification to understand the role played by stretch reflexes and joint mechanics in the control of posture and movement; and the development of bioinformatics tools and techniques for proteomics.

Dr. Kearney is active with the IEEE Engineering in Medicine and Biology Society serving as President of the Society in 1998 and co-chairing the Society's 2001 Annual Conference in Istanbul, Turkey. He is a Fellow of the Engineering Institute of Canada and the American Institute of Medical and Biological Engineering. He is a recipient of the IEEE Millennium medal.